Gas-Phase Reactions of Nickel and Nickel Oxide Clusters with Nitrogen Dioxide. 4. Continued Kinetic and Mechanistic Investigation of Nickel Cluster Reactions with NO_x Gases

W. D. Vann and A. W. Castleman, Jr.*

Department of Chemistry, Pennsylvania State University, 152 Davey Laboratory, University Park, Pennsylvania 16802

Received: September 16, 1998; In Final Form: December 10, 1998

Results of investigations of the gas-phase reactions of nickel and nickel oxide ions with NO_2 are reported in this final part of a four-part series. A fast flow reactor−quadrupole mass spectrometer system coupled with a laser vaporization source is used to study reactions of nickel and nickel oxide cluster ions with nitrogen dioxide. Pseudo-first-order bimolecular rate constants for the reactions of NO_2 with nickel and nickel oxide cluster cations and anions are reported. The product distributions indicate that several different reaction mechanisms occur between NO_2 and various sizes of nickel and nickel oxide cluster ions. The reaction processes are mainly oxidation of the nickel clusters and NO_2 addition. Finally, a detailed comparison is made between these reactions and previously reported ones with nitric oxide and oxygen.

I. Introduction

A considerable amount of research has been conducted over the past several decades, utilizing cluster chemistry to probe many different areas of chemistry.[1] For example, in terms of unraveling the details of various catalytic processes, cluster chemistry allows intermediate reaction processes and short-range interactions between the catalyst and the reactants to be studied in the gas phase. Indeed, reaction mechanisms, reaction rates, competing reactions, and poisoning processes can be examined in detail through the use of cluster chemistry. Many metal[2] and metal oxide[3] cluster systems have been used to provide useful information for interactions occurring between a catalyst and reactant. Recently, Shi and Ervin reported a gas-phase catalytic cycle for the oxidation of carbon monoxide by platinum cluster anions.[4] The fast flow reactor systems used both by Ervin et al. and in the studies reported here provide an intermediate pressure step between surface studies, which are typically conducted under conditions of high vacuum, and actual catalytic processes.

Reactions of both nickel and nickel oxide ion clusters have been reported previously with nitric oxide.[5−7] The present paper focuses on gas-phase reactions of nickel and nickel oxide cluster ions with nitrogen dioxide under well-defined thermal conditions at intermediate pressures. To study these reactions, nickel and nickel oxide cluster ions are produced by laser vaporization, reacted in a fast flow reactor, and then detected by a quadrupole mass spectrometer. The present experiments reveal new information on reactions, reaction rates, and reaction mechanisms occurring between nickel and nickel oxide cluster ions and nitrogen dioxide.

II. Experimental Section

The fast flow reactor mass spectrometer used in this work has been described in detail previously.[7,8] Briefly, a translating and rotating nickel rod is vaporized in the presence of a flowing stream of helium carrier gas. Laser vaporization is performed using the second harmonic of a Nd:YAG laser. Adding small amounts of oxygen to the carrier gas produces nickel oxides. The continuous flow of He (9000 sccm) carries the ablated species out of the source through a conical nozzle and into the flow tube. As the ions are carried through the flow tube, they are thermalized (296 K) by collisions with the carrier gas, which is maintained at a pressure of around 300 mTorr. Neutral reactant gas (NO_2) is added through a reactant gas inlet and is allowed to react with the cluster ions for a measured amount of time before being sampled into a quadrupole mass filter and detected by a channel electron multiplier.

III. Results and Discussion

Nickel and Nickel Oxide Cluster Reactants. Nickel and nickel oxide cluster ions are formed by laser vaporization of a nickel rod. An example of each of these four different types of reactant cluster distributions is shown in Figure 1. Several of the more prominent peaks are labeled as Ni_x or Ni_xO_y, but for clarity only a limited number of the peaks are labeled in the figure. The mass assignments of most of the unmarked peaks in Figure 1 can be determined by adding or subtracting oxygen (16 amu) from those peaks labeled in each of the spectra. Also, the spectra are vertically aligned so that the peaks marked in spectra a and b of Figure 1 (nickel cation and anion clusters) coincide with each other, as do the marked peaks in spectra c and d of Figure 1 (nickel oxides). The spectra show nickel clusters to Ni_{13} and nickel oxide clusters to $Ni_{10}O_{11}^+$ for cations and to $Ni_9O_{14}^-$ for anions. Some smaller oxides (Ni_xO and Ni_xO_2) are observed in both the cation and anion nickel spectra (spectra a and b of Figure 1). The amount of oxides in the nickel distribution (spectra a and b of Figure 1) can be reduced by an extended period of ablation to remove surface oxides from the nickel rod. But some oxides arise from minute leakage of air into the laser vaporization source at the O-ring seal that allows the nickel rod to be rotated and translated. Nickel cation clusters do not oxidize as readily at the laser vaporization source as do the nickel anion clusters. This can be seen by a comparison of spectra a and b of Figure 1, both of which are produced under

10.1021/jp9837479 CCC: $18.00

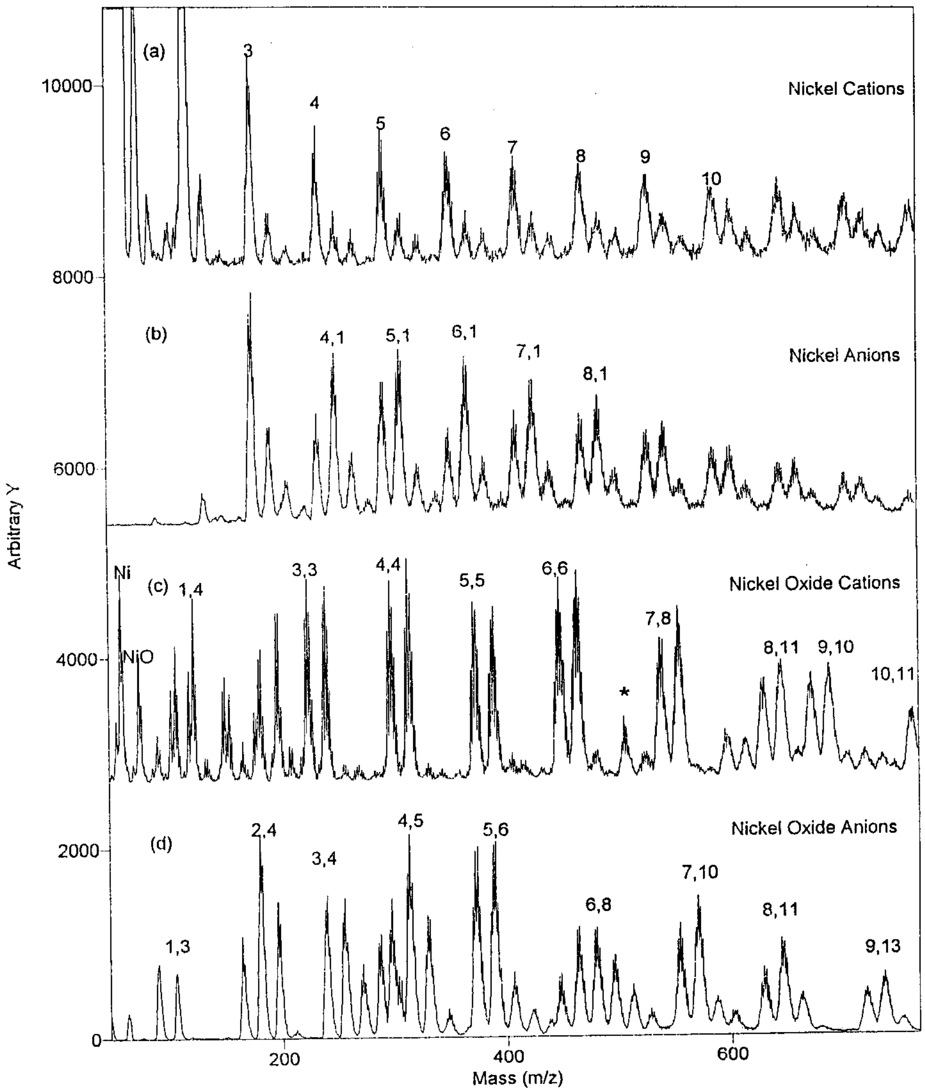

Figure 1. Nickel and nickel oxide reactant ion cluster distributions, labeled as Ni_xO_y: (a) nickel cation clusters; (b) nickel anion clusters; (c) nickel oxide cation clusters; (d) nickel oxide anion clusters.

the same experimental conditions. The nickel anion spectrum contains considerably more Ni_xO and Ni_xO_2 clusters. The anion spectrum also contains no significant nickel monomer or dimer clusters (only a slight amount of NiO_2^- and Ni_2O^-). This is very typical of nickel anion distributions and perhaps indicates that the electron attachment rates to the monomer and dimer are sufficiently slower than the electron attachment rates for the trimer and larger clusters. The electron affinities for these nickel clusters increase gradually from the monomer (1.156 eV)[9] and dimer (0.926 eV)[10] to the trimer (1.41 eV)[11] and larger clusters (1.5−3.0 eV).[12,13] It may also be possible that nickel anion clusters have faster electron attachment rates when oxygen is added to the cluster, since small amounts of NiO_2^- and Ni_2O^- are often seen with the normal nickel anion distribution, but the monomer and dimer bare anions are never observed. In Figure 1a (cations), the nickel monomer and dimer are off scale compared to the trimer and other larger clusters. The dimer is a factor of 5 times larger than the trimer, and the monomer is 20 times larger. It is interesting to note that the monomer and dimer clusters produce disproportionately smaller cation oxide clusters when compared to the oxides produced by the larger cation clusters. The nickel monomer is the first peak observed in Figure 1c; the next three peaks are NiO^+, NiO_2^+, and NiO_3^+.

The two nickel oxide spectra (spectra c and d of Figure 1), each produced by adding 1 sccm of oxygen to the carrier gas at the laser vaporization source, are seen to contain many of the same species. However, the nickel oxide anion species are slightly more oxidized by this small concentration of oxygen added at the source. For instance, $Ni_3O_3^+$ and $Ni_3O_4^+$ species are produced upon reacting nickel cations with 1 sccm of oxygen, but for anions the $Ni_3O_4^-$, $Ni_3O_5^-$, and $Ni_3O_6^-$ are produced by the same reaction. This shift to higher oxides for anions can be observed throughout the entire distribution. The species marked with an asterisk in Figure 1c is a somewhat anomalous peak for a nickel oxide spectrum. This cluster is $Ni_7O_6^+$ and is the only nickel-rich nickel oxide observed in either of the two nickel oxide distributions. This further illustrates the fact that nickel cations take up oxygen more slowly than nickel anion clusters. The fact that nickel anions saturate with oxygen more readily (i.e., at lower concentrations of O_2) is in agreement with previously reported reaction rates for oxygen with anionic[6,14] and cationic[5] nickel clusters.

Nickel Cluster Cation Reactions. Nitrogen dioxide was reacted with nickel cluster cation distributions such as the one shown in Figure 1a. These reactions produced three main types of products, namely, oxidation of the nickel clusters, addition of nitric oxide, and addition of nitrogen dioxide to the nickel and newly formed nickel oxide clusters. Figure 2 shows several product distributions for the reaction of nickel cations with nitrogen dioxide. The lower spectrum displays the nickel cluster

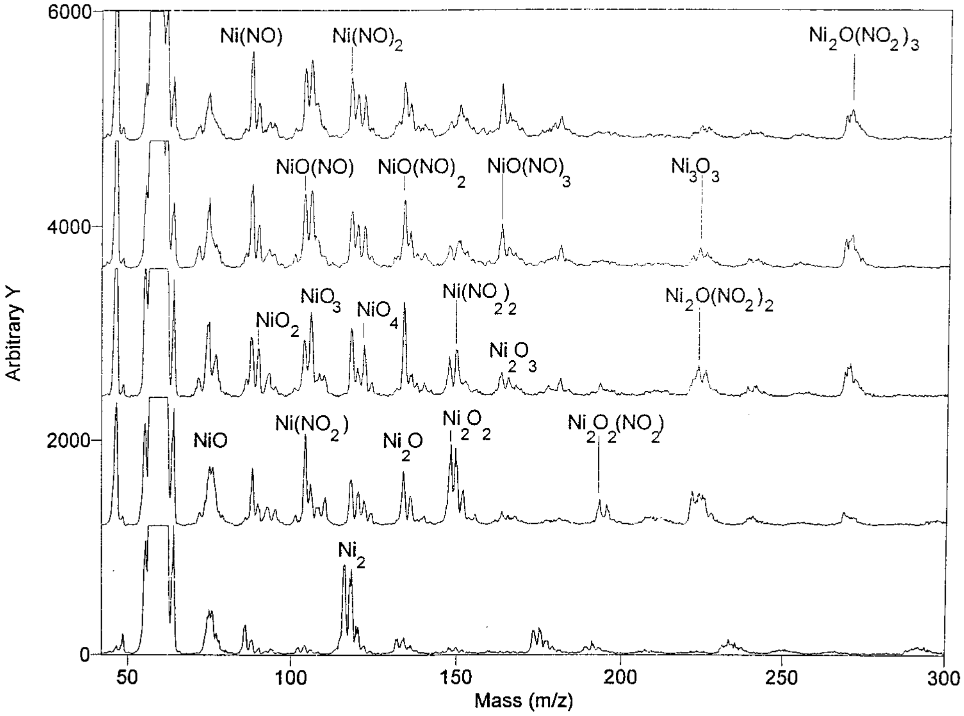

Figure 2. Nickel cation product distributions for the reaction of NO_2, showing mainly nickel monomer and dimer cluster species. The bottom spectrum is nickel cation reactant distribution. The upper four spectra are for increasing concentrations of NO_2 (0, 1, 2, 3, and 4 sccm from bottom to top, respectively).

starting materials. The next spectrum up is obtained with 1 sccm of nitrogen dioxide added. Each of the successive spectra is for 2, 3, and 4 sccm of nitrogen dioxide, respectively. Figure 2 shows mainly the reaction products for the nickel monomer and dimer cations, which tend to react somewhat differently than the larger nickel clusters. Many different product species are labeled throughout the spectra. Nickel clusters are oxidized, forming NiO_2, NiO_3, Ni_2O, and Ni_2O_2. Further, addition products of nitrogen dioxide and nitric oxide are both observed in several of the monomer cluster species. The formation of nitric oxide by the reduction of nitrogen dioxide in the presence of the nickel clusters is evident by the many nitric oxide addition species seen in the spectra. Also, the observed oxidation of nickel clusters by nitrogen dioxide is further supporting evidence that nitrogen dioxide is being reduced by the nickel clusters. It is not surprising that nitrogen dioxide would be reduced in the process of oxidizing nickel clusters, since this same oxidation process is observed from the reaction of nickel clusters with nitric oxide. Although it is possible that the product of this reduction process (nitric oxide) reacts efficiently enough to compete with the extremely more abundant nitrogen dioxide to form NO addition products, it does not seem likely considering the relative concentrations of NO_2 and NO. Nitrogen dioxide is added at concentrations of 10^{11} molecules cm^{-3}, whereas the concentrations of cluster ions are at least 3−4 orders of magnitude lower, and furthermore, the concentration of NO produced by these cluster ions should be even lower. A more likely alternative to the explanation of the presence of nitric oxide in the product distributions is that nitrogen dioxide bonds with the nickel cluster species and an oxygen atom is lost from the cluster. This is a more reasonable possibility, considering that in reactions with nickel oxide cation clusters, nitric oxide was observed to replace oxygen on the cluster. In other words, in the case of the monomer, nitric oxide may bond more strongly or more readily to the nickel clusters than oxygen.

Figure 3 shows several product distributions of different nitrogen dioxide concentrations. In this figure, mainly the reaction products of the dimer and trimer are displayed. The lower spectrum is for 1 sccm of nitrogen dioxide addition, and each successive spectrum is for an increasing concentration of NO_2 (2, 3, 4, 5, 6, and 8 sccm, respectively). Two main reaction processes are seen to occur in these spectra. First, oxidation of the nickel clusters is observed from the reaction of 1−3 sccm of NO_2. In this particular mass region of the spectra the formation of Ni_2O^+, $Ni_2O_2^+$, Ni_3O^+, $Ni_3O_2^+$, $Ni_3O_3^+$, Ni_4O^+, and $Ni_4O_2^+$ are all observed, and it appears that the oxidation process truncates at stoichiometric nickel oxide clusters. The second type of reaction occurring between nickel cations and nitrogen dioxide is seen at increased reactant concentrations. This product is the addition of NO_2 on the stoichiometric product nickel oxides. This final addition process yields cluster species such as $Ni_2O_2(NO_2)^+$ and $Ni_3O_3(NO_2)^+$ labeled as 2,2,1 and 3,3,1 in the top spectrum in Figure 3. With the possible exception of the nickel monomer as seen in Figure 2, no nitrogen dioxide addition to bare nickel clusters is observed at any point throughout the entire product distributions. The possible exception found with the nickel monomer, such as the $Ni(NO_2)$ cluster, cannot be unambiguously assigned. In Figure 2 this product peak is labeled both as $Ni(NO_2)$ and NiO(NO); indeed, there is no way to distinguish between these two products. The same is also true for the species labeled $Ni(NO_2)_2$ in Figure 2.

These same two reaction processes (oxidation and addition) are observed in the higher mass region of the product distributions and are shown in Figure 4. These larger nickel clusters both oxidize and add nitrogen dioxide. One significant difference that occurs at these larger clusters is the addition of nitrogen dioxide after only one oxygen is added to the bare nickel clusters, and once one nitrogen dioxide is added, these clusters continue to add oxygen. For instance, as the NO_2 concentration is increased, $Ni_4O(NO_2)^+$ (labeled as 4,1,1 in the figure) becomes $Ni_4O_2(NO_2)^+$ (marked with asterisk, third spectrum from the top) and then $Ni_4O_3(NO_2)^+$ (marked with asterisk, second spectrum from the top). Cluster species such as these are marked with asterisks in Figure 4 in order to keep the figure

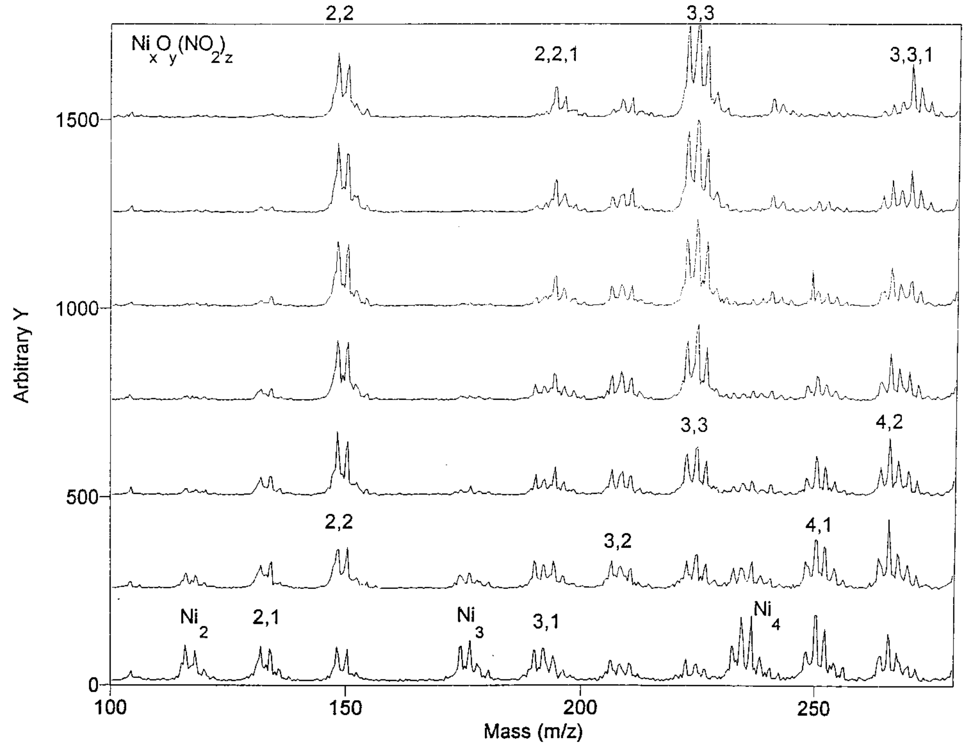

Figure 3. Product distributions for the low-mass region of the spectra for the reaction of $Ni_x^+ + NO_2$. From bottom to top, the spectra are for increasing concentrations of NO_2 (1, 2, 3, 4, 5, 6, and 8 sccm, respectively). Both oxidation of nickel cluster and addition of NO_2 are observed.

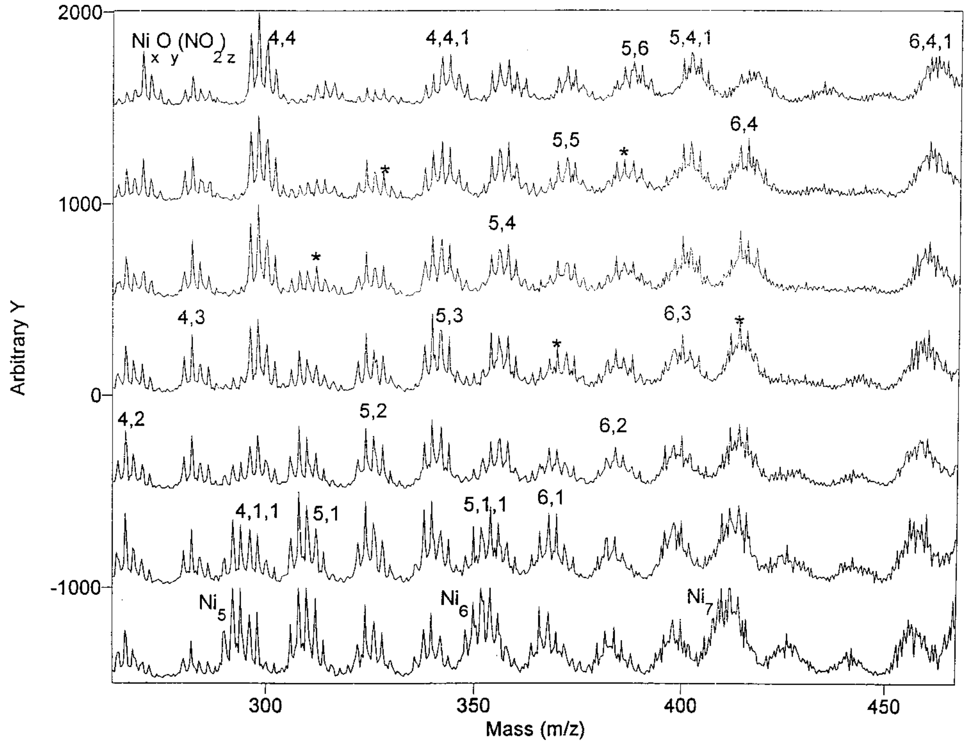

Figure 4. High-mass product distributions for the reaction of $Ni_x^+ + NO_2$. From bottom to top, the spectra are for increasing concentrations of NO_2 (1, 2, 3, 4, 5, 6, and 8 sccm, respectively). Both oxidation of nickel cluster and addition of NO_2 are observed. Asterisks indicate the series $Ni_xO_z(NO_2)$ where $x = 4$, 5, or 6 and $z = 1$, 2, or 3.

from being overly crowded with labeling. The rightmost asterisk in the middle spectrum indicates 6,1,1, and in this series no other oxygen additions are observed. An interesting anomaly is observed at the far right of the 4, 5, and 6 sccm spectra, namely, the region of the spectra (approximately 40 amu wide) where there are no product species. This can be attributed to the two reaction processes previously discussed. To reiterate, at these concentrations, the Ni_7^+ clusters have oxidized to form clusters of higher mass and these do not contribute to any product species in the mass range under consideration, and the Ni_6^+ clusters have formed oxides up to $Ni_6O_4^+$. At this point, the first addition of nitrogen dioxide occurs, forming the $Ni_6O_4(NO_2)^+$ cluster. It is this jump from the $Ni_6O_4^+$ to the $Ni_6O_4(NO_2)^+$ that causes the absence of product species in this region of the spectra. There is a slight indication of the same kind of jump occurring between $Ni_4O_4^+$ and $Ni_4O_4(NO_2)^+$ in the top

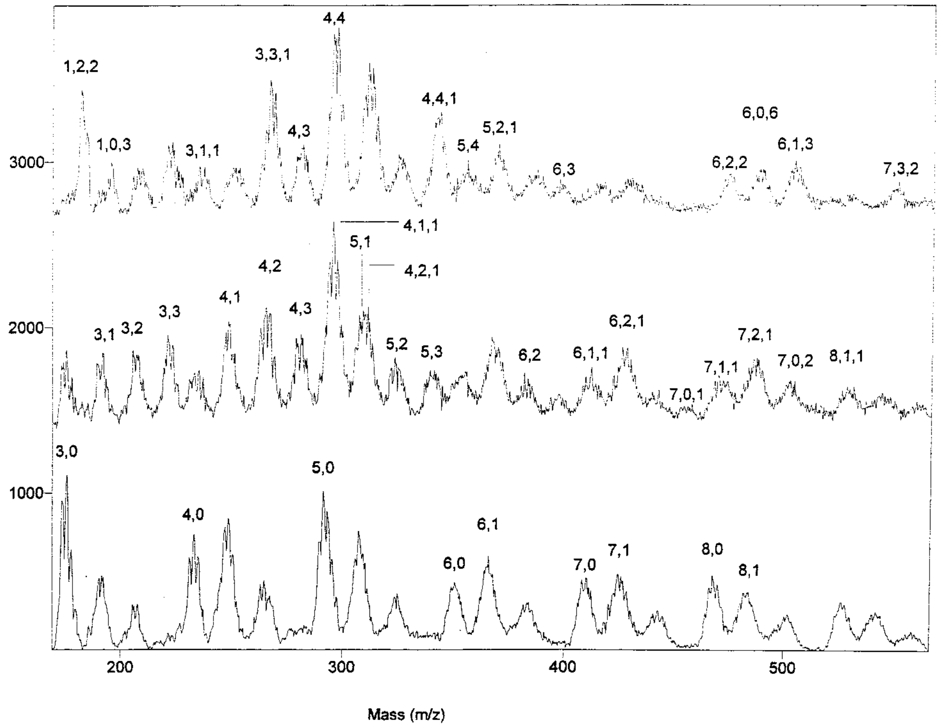

Figure 5. Product distributions for the reaction of $Ni_x^- + NO_2$ at low concentrations. The bottom spectrum is the nickel anion reactant distribution. The middle spectrum is for 0.2 sccm of NO_2; the top spectrum is for 0.5 sccm of NO_2. Clusters are labeled as $Ni_xO_y^-$ and $Ni_xO_y(NO_2)_z^-$. Oxidation of nickel anion clusters and addition of NO_2 are observed.

spectrum. In these product distributions there is an overall shift to higher masses as products are being formed, which is not always observed in the product distributions that will be discussed in the following sections. This shift to higher mass products is indicative of an overall addition process and the absence of cluster fragmentation as a dominant process.

Nickel Cluster Anion Reactions. The reactions of nickel anion clusters produce many of the same products as are observed with nickel cation clusters. The same reaction processes are occurring, namely, oxidation of the nickel clusters and addition of nitrogen dioxide to the nickel oxide clusters. In addition, nitrogen dioxide is observed to add directly to bare nickel anion clusters such as those seen in Figure 5. In this figure, the bottom spectrum is the nickel and nickel-rich oxide starting material. The middle spectrum is for 0.2 sccm nitrogen dioxide and the top spectrum for 0.5 sccm. Considering the wide variety of product species found in each of these distributions, it appears that oxidation and addition processes occur competitively; that is, they appear to be proceeding at roughly the same rate. This is a significant difference compared to what was found for cation reactions, which appear to oxidize more rapidly than they add nitrogen dioxide.

Figure 6 shows nickel anion reactions at higher concentrations and enables the trimer and tetramer product formation processes to be traced. At 1 sccm of nitrogen dioxide, the trimer and tetramer clusters are fully oxidized and have each added nitrogen dioxides to the cluster. The trimer continues to add one more nitrogen dioxide and truncates at $Ni_3O_3(NO_2)_3^-$. The tetramer continues to add nitrogen dioxides up to $Ni_4O_4(NO_2)_6^-$. The nickel cluster species from the pentamer and higher do not appear to react in the same manner as do the nickel trimer and tetramer. There are very little $Ni_xO_y(NO_2)_z^-$ cluster species with x greater than or equal to 5. This is the opposite of what was observed for the nickel cation reactions where a definite shift to higher masses indicated a simple addition process with little or no fragmentation of the larger clusters.

The two high-intensity peaks growing in the far left of the spectra are the $NiO_2(NO_2)_3^-$ and the $NiO_3(NO_2)_3^-$. It is apparent that these two product species are produced from higher mass clusters because nickel anion cluster distributions produce very little if any nickel monomer anion starting material. This observation, together with the absence of higher mass nickel oxide product species, indicates that as these larger clusters react with nitrogen dioxide, the cluster is fragmented, leaving the monomer oxide addition species.

The low-mass region of the spectra not shown in Figure 6 contains a large amount of NO_2^-; this species appears even at the lowest concentration added. This peak intensity is approximately 6 times the intensity of the nickel pentamer shown in the bottom spectrum in Figure 6. It has an intensity comparable with that of the $NiO_2(NO_2)_3^-$ at 20 sccm (see top spectrum in Figure 6). At the lowest concentrations of NO_2 (0.5 sccm) a smaller NO_3^- species appears with about one-fifth the intensity of the NO_2^- ion. As the concentration increases to 10 sccm, the intensity of the NO_3^- becomes comparable with the intensity of NO_2^-.

At concentrations of 10 sccm and greater, molecular ion clusters of NO_2 and NO_3 are observed at intensities of one-quarter to two-thirds the intensity of the NO_2^- ion. The molecular cluster are dimers ($(NO_2)_2^-$ and $(NO_3)_2^-$) and a trimer ($(NO_2)_3^-$) as well as a mixed cluster ion ($NO_2{\cdot}NO_3^-$). Each of these ions are of stronger intensities than all the nickel cluster ions shown in Figure 6 with the exception of the $NiO_2(NO_2)_3^-$. The presence of these large molecular cluster ions indicates that a charge-transfer reaction is occurring between the nickel and nickel oxide cluster ions, and the neutral NO_2 reactant gas. This is not surprising when one considers the electron affinity of NO_2, which is 2.3 eV,[15] and the electron affinity of the nickel clusters, such as the trimer at 1.4 eV[11] and the hexamer at 1.9 eV.[12]

Nickel Oxide Cluster Cation Reactions. Nickel oxide cluster cation distributions such as the one shown in Figure 1c were

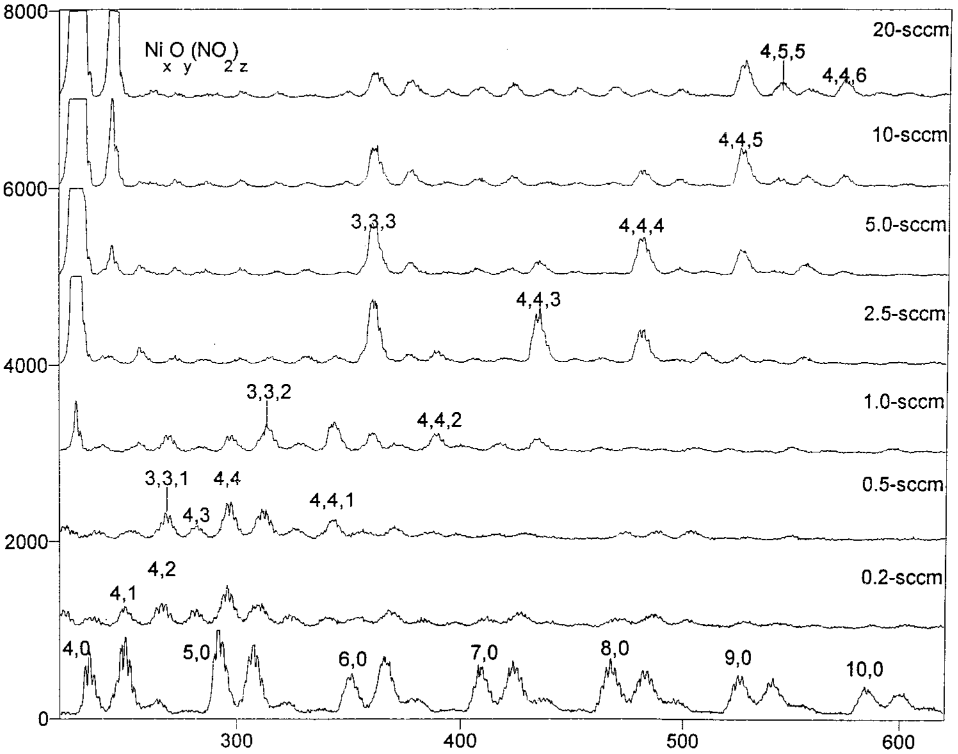

Figure 6. Product distributions for the reaction of $Ni_x^- + NO_2$ at higher concentrations. The bottom spectrum is nickel anion reactant distribution. From bottom to top, the spectra are for increasing concentrations of NO_2 (0, 0.5, 1.0, 2.5, 5.0, 10, and 20 sccm, respectively). The clusters quickly oxidize at concentrations below 0.5 sccm of NO_2. With increasing concentrations, stepwise addition of NO_2 can be followed.

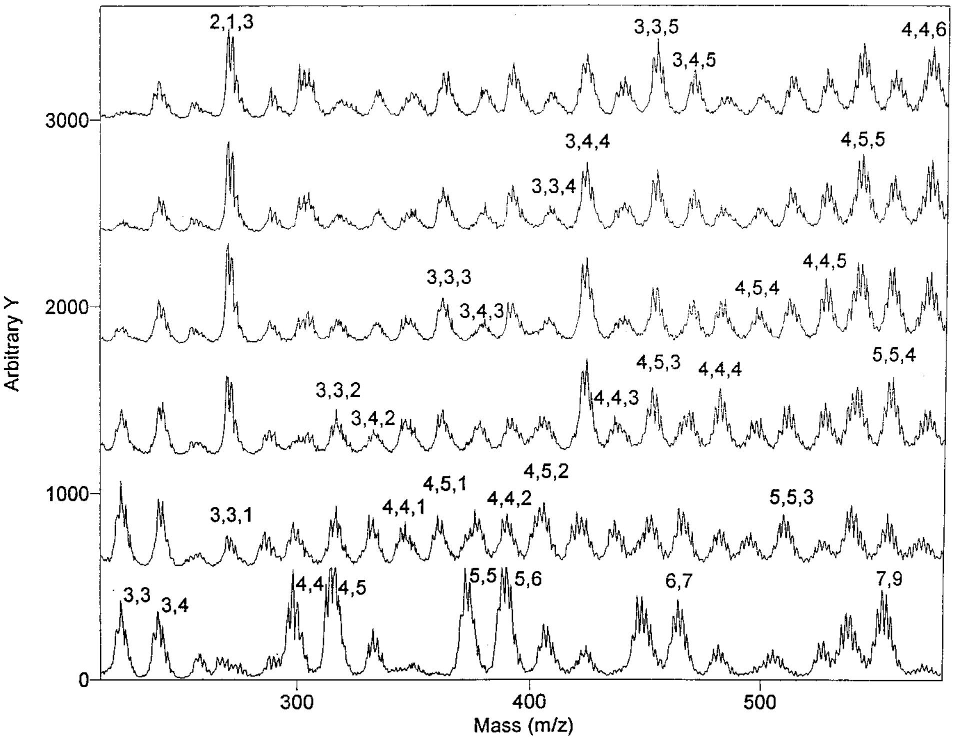

Figure 7. Product distributions for the reaction of $Ni_xO_y^+ + NO_2$. From bottom to top, the spectra are for increasing concentrations of NO_2 (0, 0.5, 1.25, 2.5, 3.75, and 5.0 sccm, respectively). A stepwise addition process can be observed from these reactions.

also reacted with nitrogen dioxide. Figure 7 shows several product distributions (top five spectra) and a nickel oxide reactant distribution (bottom spectrum). Again, each of the product distributions is for increasing concentrations of NO_2. From bottom to top, the concentration of NO_2 added to produce each spectrum is 0, 0.5, 1.25, 2.5, 3.75, and 5 sccm, respectively. The figure shows that with increasing concentration, consecutive additions of NO_2 can be followed. For instance, the $Ni_3O_3^+$ (labeled as 3,3 in Figure 7) at 0.5 sccm forms $Ni_3O_3\ (NO_2)^+$ and at 1.25 sccm the $Ni_3O_3\ (NO_2)_2^+$ cluster is formed. At higher concentrations, the product distribution shows the further formation of $Ni_3O_3\ (NO_2)_3^+$, $Ni_3O_3\ (NO_2)_4^+$, and finally Ni_3O_3

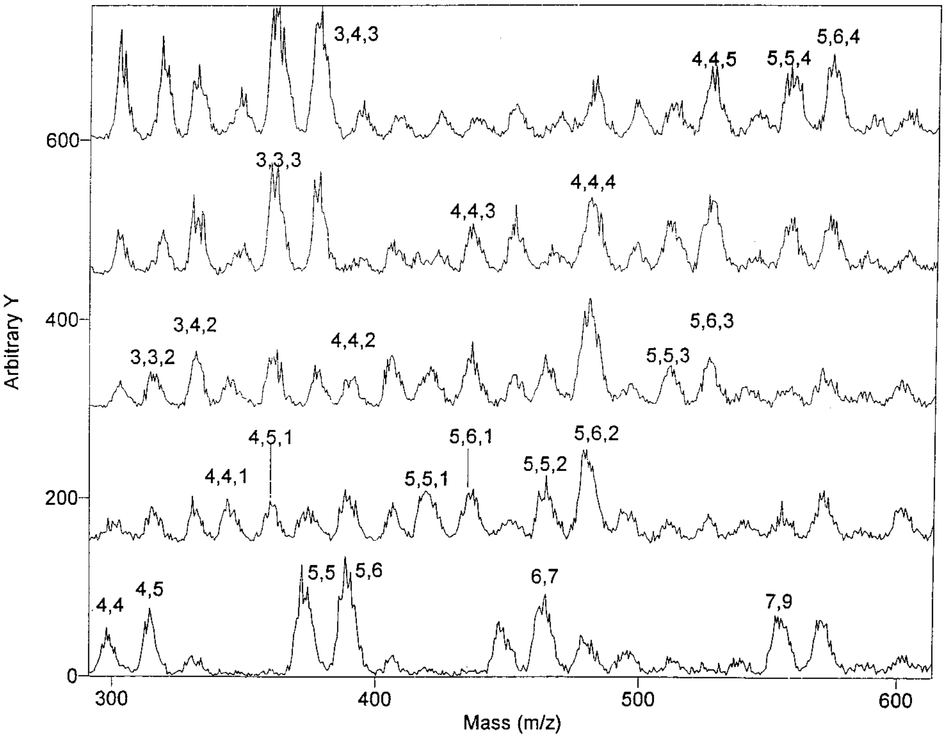

Figure 8. Product distributions for the reaction of $Ni_xO_y^- + NO_2$. From bottom to top, the spectra are for increasing concentrations of NO_2 (0, 0.5, 1.0, 2.5, and 5.0 sccm, respectively). A stepwise addition process can be observed from these reactions.

$(NO_2)_5^+$. The same consecutive additions on the nickel oxide cluster starting material can be followed in the figure for the $Ni_3O_4^+$, $Ni_4O_4^+$, $Ni_4O_5^+$, and $Ni_5O_5^+$ species. This addition process is fairly straightforward with only a few interesting occurrences.

There is some evidence of further oxidation processes occurring from these reactions. For instance, the peak labeled 4,4,1 in Figure 7 accounts for only part of this species. This grouping of isotopes spans a larger mass region than it should, indicating the presence of another species of slightly higher mass. This second cluster species appears to be $Ni_4O_7^+$. This newly formed oxide can also be seen to add NO_2 stepwise, as do the other oxides in the distribution. This same argument reveals the possibility of a $Ni_3O_6^+$ cluster partially overlapping with the 3,3,1 cluster.

A careful inspection of the spectra in Figure 7 reveals that the $Ni_3O_3(NO_2)_3^+$, $Ni_3O_4(NO_2)_4^+$, $Ni_4O_4(NO_2)_4^+$, and $Ni_4O_5(NO_2)_5^+$ are slightly more prominent than many of the species around them. From this, it appears that there is some connection between the oxygen in the cluster and how many nitrogen dioxides the cluster may prefer to add. Also, it appears that the $Ni_3O_3(NO_2)_5^+$ cluster is more prominent than the $Ni_3O_3(NO_2)_4^+$ cluster. This suggests that for some reason the 3,3,5 cluster is more stable than the 3,3,4 cluster. Such an occurrence is not observed for the 4,4,5 and 4,4,6 clusters, which are both prominent species in the spectra. The one anomalous peak seen in the figure is the 2,1,3 cluster, which may not be produced by a simple addition process. This conclusion is based on the fact that there does not appear to be sufficient nickel dimer oxide starting material to have produced this amount of the 2,1,3 cluster.

Nickel Oxide Cluster Anion Reactions. The final set of reactions is for $Ni_xO_y^-$ clusters and NO_2. Figure 8 shows how similar processes occur with nickel oxide anions as with nickel oxide cations. The bottom spectrum is nickel oxide anion starting material. From bottom to top, the next four spectra are for the addition of 0.5, 1.0, 2.5, and 5 sccm of neutral NO_2 reactant gas. Consecutive additions on the nickel oxide anion species shown in the figure can again be followed as NO_2 concentration is increased. For example, the reaction of $Ni_4O_4^-$ cluster with 0.5 sccm of NO_2 first forms $Ni_4O_4(NO_2)^-$. Then the formation of $Ni_4O_4(NO_2)_2^-$ is found to proceed at 1.0 sccm. At 2.5 sccm, both the $Ni_4O_4(NO_2)_3^-$ and $Ni_4O_4(NO_2)_4^-$ are observed in the spectrum, and finally, at higher concentrations the $Ni_4O_4(NO_2)_5^-$ cluster is seen growing in. In these distributions it is difficult to discern any unusually prominent species. The $Ni_3O_3(NO_2)_3^-$ and $Ni_3O_3(NO_2)_4^-$ clusters appear to be somewhat more prominent than some of the higher mass clusters; at 0.5 and 1.0 sccm the $Ni_5O_6(NO_2)_2^-$ cluster appears to be particularly more prominent than all other clusters in the distributions.

Figure 9 shows a larger region of the mass spectrum of the product distribution for this same reaction taking place at 5 sccm. This is the same spectrum as shown at the top of Figure 8. This expanded view shows the existence of $NiO_2(NO_2)_3^-$, $Ni_2O_3(NO_2)_2^-$, and $Ni_2O_4(NO_2)_2^-$ clusters, which cannot be seen in Figure 8. The two main points of this figure are the extremely high relative intensity of the $NiO_2(NO_2)_3^-$ cluster and the lack of any significant clusters below this mass. First, the relatively high intensity of the $NiO_2(NO_2)_3^-$ cluster compared to the other clusters in the distribution indicates this species to be a preferred product of this reaction. This same species was also a preferred product from the $Ni_x^- + NO_2$ reactions (see Figure 6). In each of these two distributions, this cluster ion is considerably more prominent than other nickel oxide/nitrogen dioxide clusters. Second, there are no molecular anion clusters $(NO_2)_x(NO_3)_y^-$ occurring with the nickel oxide anion reactions, indicating the absence of a charge-transfer process, which does occur in the reactions of nickel cluster anions with nitrogen dioxide. This is not, however, a surprising result considering that increasing the oxygen content of the cluster might be expected to increase its electron affinity.

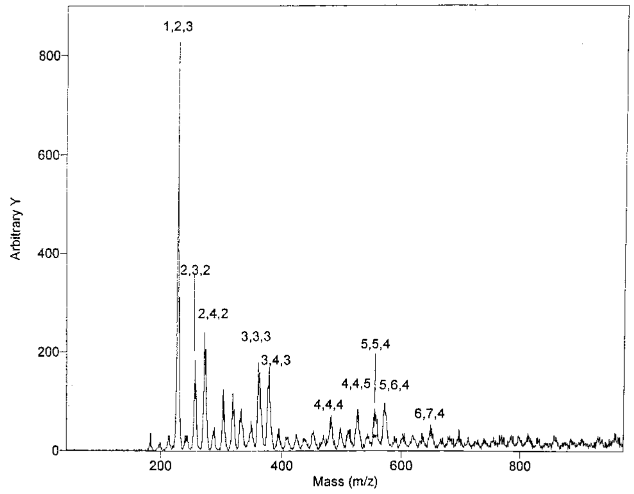

Figure 9. Product distribution for the reaction of $Ni_xO_y^- + NO_2$. This is the same spectrum as the highest concentration shown in Figure 8. This expanded view shows a magic cluster ($NiO_2(NO_2)_3^-$) and a lack of any significant clusters below this point in the spectrum.

Kinetic Data. Kinetic analysis of nickel and nickel oxide cluster ion reactions with NO_2 were performed. Pseudo-first-order bimolecular rate constants for the reactions

$$Ni_x^+ + NO_2 \rightarrow\rightarrow Ni_xO_y(NO_2)_z^+ + \text{neutrals} \qquad (1a)$$

$$Ni_x^- + NO_2 \rightarrow\rightarrow Ni_xO_y(NO_2)_z^- + \text{neutrals} \qquad (1b)$$

$$Ni_xO_y^+ + NO_2 \rightarrow\rightarrow Ni_xO_y(NO_2)_z^+ + \text{neutrals} \qquad (1c)$$

$$Ni_xO_y^- + NO_2 \rightarrow\rightarrow Ni_xO_y(NO_2)_z^- + \text{neutrals} \qquad (1d)$$

are obtained from the slopes of semilog plots through the relation

$$\ln(I/I_o) = -k[NO_2]t \qquad (2)$$

where I/I_o is the intensity of the reactant cluster ions (Ni_x^+, Ni_x^-, $Ni_xO_y^+$, or $Ni_xO_y^-$) at given concentrations of NO_2 divided by the intensity of these same species at zero NO_2 concentration, k is the rate constant, and t is the reaction time (4.2 ms measured by pulsing experiments).[16] For each reaction spectrum at a given concentration, one or more reference spectra (i.e., zero-concentration spectra) are taken.

The reaction rates for the reactions given in Tables 1−4 were determined by averaging several different data sets in order to eliminate scan-to-scan fluctuations in the data. Most reactant cluster ions overlap with reaction product ions at least to some degree. This not only reduced the number of measurable reaction rates but also contributed to experimental error in the reported rates by limiting the amount of data obtained. The reaction rates reported were obtained from measurements of starting material isotopes that did not overlap with product ions. These isotopes were often considerably less intense than the main isotopes of the nickel cluster reactants, and higher peak intensity yielded rate constants with smaller errors. Sufficiently high signal intensity is needed for the determination of reaction rates, and increasing resolution in order to differentiate isotopes dramatically reduced the available signal intensity.

All reaction rates that could be obtained without interference from product overlap are reported in Tables 1−4. Rate constants for larger reactant cluster species were not reported because of lower concentrations of these species. In addition to reaction rates, calculated collision rates (Langevin limit with Su−Chesnavich parametrization for polar molecules)[17] are provided in each table. A comparison of these collision rates with the experimentally determined rates gives an indication of the efficiency of the reactions. Also, where available, previously reported reaction rates for the reaction of nitric oxide with each different cluster ion species are listed to provide a comparison of the two reactions. The reaction rates of nitrogen dioxide reaction with nickel clusters cations are given in Table 1. Table 2 lists the reaction rates for nickel cluster anions with nitrogen dioxide, while Tables 3 and 4 give the rate constants for the reactions of nitrogen dioxide with nickel oxide cation and anion clusters, respectively.

It is interesting to compare the reaction rates of NO_2 with reaction rates for the similar reactions with nitric oxide. Figures 10 and 11 compare the rates reported in Tables 1−4 with each other and for reactions of nitric oxide with the various nickel and nickel oxide clusters. Also, the reaction rates of oxygen are included in the comparison of the reaction rates with nickel anion clusters because of the interesting similarities found in their respective rate constants. Figure 10a gives the comparison

TABLE 1: NO_2 Reactions with Nickel Cluster Cations

reaction	exptl rate constant ($10^{-10}cm^3s^{-1}$)	calcd NO_2 collision rate (10^{-9} cm^3 s^{-1})	NO reaction rate constant (10^{-10} cm^3 s^{-1})
$Ni_2^+ + NO_2 \rightarrow\rightarrow Ni_2O_x(NO_2)_y^+$	7.7 ± 0.8	2.58	1.2 ± 0.2
$Ni_3^+ + NO_2 \rightarrow\rightarrow Ni_3O_x(NO_2)_y^+$	8.7 ± 1.3	2.46	2.1 ± 0.2
$Ni_4^+ + NO_2 \rightarrow\rightarrow Ni_4O_x(NO_2)_y^+$	9.8 ± 1.2	2.39	7.8 ± 0.8
$Ni_5^+ + NO_2 \rightarrow\rightarrow Ni_5O_x(NO_2)_y^+$	10.7 ± 2.4	2.35	8.3 ± 0.8
$Ni_6^+ + NO_2 \rightarrow\rightarrow Ni_6O_x(NO_2)_y^+$	10.6 ± 2.3	2.33	6.6 ± 0.9
$Ni_7^+ + NO_2 \rightarrow\rightarrow Ni_7O_x(NO_2)_y^+$	8.1 ± 1.4	2.31	7.1 ± 0.9
$Ni_8^+ + NO_2 \rightarrow\rightarrow Ni_8O_x(NO_2)_y^+$	8.3 ± 1.9	2.29	4.7 ± 0.8

TABLE 2: NO_2 Reactions with Nickel Cluster Anions

reaction	exptl rate constant (10^{-10} cm^3 s^{-1})	calcd NO_2 collision rate (10^{-9} cm^3 s^{-1})	NO reaction rate constant (10^{-10} cm^3 s^{-1})
$Ni_3^- + NO_2 \rightarrow\rightarrow Ni_3O_x(NO_2)_y^-$	7.0 ± 1.0	2.46	3.1 ± 0.3
$Ni_4^- + NO_2 \rightarrow\rightarrow Ni_4O_x(NO_2)_y^-$	6.5 ± 1.3	2.39	4.3 ± 0.2
$Ni_5^- + NO_2 \rightarrow\rightarrow Ni_5O_x(NO_2)_y^-$	5.1 ± 0.9	2.35	4.1 ± 0.2
$Ni_6^- + NO_2 \rightarrow\rightarrow Ni_6O_x(NO_2)_y^-$	4.4 ± 2.4	2.33[9]	3.6 ± 0.2
$Ni_7^- + NO_2 \rightarrow\rightarrow Ni_7O_x(NO_2)_y^-$	6.2 ± 1.3	2.31	4.1 ± 0.4
$Ni_8^- + NO_2 \rightarrow\rightarrow Ni_8O_x(NO_2)_y^-$	6.7 ± 1.1	2.29	4.2 ± 0.3
$Ni_9^- + NO_2 \rightarrow\rightarrow Ni_9O_x(NO_2)_y^-$	5.1 ± 0.7	2.28	3.6 ± 0.6

TABLE 3: NO_2 Reactions with Nickel Oxide Cluster Cations

reaction	exptl rate constant (10^{-10} cm^3 s^{-1})	calcd NO_2 collision rate (10^{-9} cm^3 s^{-1})	NO reaction rate constant (10^{-10} cm^3 s^{-1})
$Ni_4O_4^+ + NO_2 \rightarrow\rightarrow Ni_xO_y(NO_2)_z^+$	3.0 ± 0.5	2.35	2.8 ± 0.7
$Ni_4O_5^+ + NO_2 \rightarrow\rightarrow Ni_xO_y(NO_2)_z^+$	4.8 ± 1.0	2.34	8.6 ±2.1
$Ni_5O_5^+ + NO_2 \rightarrow\rightarrow Ni_xO_y(NO_2)_z^+$	5.2 ± 1.0	2.32	8.2 ± 1.0
$Ni_5O_6^+ + NO_2 \rightarrow\rightarrow Ni_xO_y(NO_2)_z^+$	4.7 ± 0.9	2.31	
$Ni_6O_6^+ + NO_2 \rightarrow\rightarrow Ni_xO_y(NO_2)_z^+$	4.8 ± 0.8	2.30	5.3 ± 0.9
$Ni_6O_7^+ + NO_2 \rightarrow\rightarrow Ni_xO_y(NO_2)_z^+$	6.2 ± 0.9	2.29	
$Ni_7O_8^+ + NO_2 \rightarrow\rightarrow Ni_xO_y(NO_2)_z^+$	5.9 ± 0.7	2.28	5.6 ± 0.8
$Ni_7O_9^+ + NO_2 \rightarrow\rightarrow Ni_xO_y(NO_2)_z^+$	5.8 ± 0.6	2.28	

TABLE 4: NO_2 Reactions with Nickel Oxide Cluster Anions

reaction	exptl rate constant (10^{-10} cm^3 s^{-1})	calcd NO_2 collision rate (10^{-9} cm^3 s^{-1})	NO reaction rate constant (10^{-10} cm^3 s^{-1})
$Ni_2O_3^- + NO_2 \rightarrow\rightarrow Ni_xO_y(NO_2)_z^-$	5.4 ± 0.9	2.47×10^{-9}	
$Ni_2O_4^- + NO_2 \rightarrow\rightarrow Ni_xO_y(NO_2)_z^-$	2.7 ± 0.8	2.45	
$Ni_3O_4^- + NO_2 \rightarrow\rightarrow Ni_xO_y(NO_2)_z^-$	4.4 ± 1.7	2.39	
$Ni_3O_5^- + NO_2 \rightarrow\rightarrow Ni_xO_y(NO_2)_z^-$	3.3 ± 1.1	2.38	
$Ni_4O_4^- + NO_2 \rightarrow\rightarrow Ni_xO_y(NO_2)_z^-$	4.1 ± 0.9	2.35	0.51 ± 0.10
$Ni_4O_5^- + NO_2 \rightarrow\rightarrow Ni_xO_y(NO_2)_z^-$	3.7 ± 0.8	2.34	1.2 ± 0.3
$Ni_5O_5^- + NO_2 \rightarrow\rightarrow Ni_xO_y(NO_2)_z^-$	3.6 ± 0.6	2.32	0.37 ± 0.13
$Ni_5O_6^- + NO_2 \rightarrow\rightarrow Ni_xO_y(NO_2)_z^-$	4.1 ± 0.8	2.31	7.1 ± 2.9
$Ni_6O_6^- + NO_2 \rightarrow\rightarrow Ni_xO_y(NO_2)_z$	$(2.8 \pm 0.7) \times 10^{-10}$	2.30×10^{-9}	$(3.7 \pm 0.6) \times 10^{-11}$

of oxygen, nitric oxide, and nitrogen dioxide with nickel cluster anions. Nickel cluster anions have been suggested (part 2 of this series[6]) to react similarly in the presence of nitric oxide and oxygen. Nitric oxide is reported to first oxidize the nickel clusters, as does oxygen. Comparing these two sets of rate constants with those of nitrogen dioxide reveals a striking similarity in their trends. This is a strong indication that, as discussed previously, oxidation is a major reaction process occurring between nitrogen dioxide and nickel anion clusters. Also, since these rates are for the initial reaction, this suggests that oxidation is the first measurable reaction. It is also interesting to note that each trend in Figure 10a shows the presence of a local minimum in the rates at the Ni_6^- cluster, indicating that the nickel hexamer anion is somewhat more stable against oxidation than many of the other cluster sizes. From Figure 10a, it also appears that Ni_3^- and Ni_9^- are somewhat less reactive to oxidation. Figure 10b shows a comparison of NO and NO_2 reacting with nickel cation clusters. Oxygen was not included in this comparison because there was no apparent correlation between its reaction rates and those of NO or NO_2. Cation reactions with oxygen did, however, show a local maximum in the rates for the hexamer.

It is somewhat more difficult to see similarities in the trends for the cation reaction rates with NO and NO_2. There is, however, a general increase to the Ni_5^+ and then a general decrease to the Ni_7^+. What is most interesting is the comparison given in Figure 10c of the nickel cations and anions reacting with nitrogen dioxide. These trends are strikingly opposite. Whatever causes the hexamer to be less reactive for anions is certainly not an important characteristic for cation reactions. This strongly indicates that the charge on the cluster plays a significant role in the rate of the reaction.

The reaction rates for nickel oxides are shown in Figure 11 comparing nitric oxide to nitrogen dioxide and cationic to anionic reactions. Figure 11a shows a comparison of NO_2 and NO with nickel oxide anions. Both of these show oscillations dependent on the ratio of oxygen to nickel in the cluster. With the exception of the pentamer oxides, these trends appear to be opposite. The reactions of NO_2 react more slowly with the more oxygen-rich cluster, and the NO appears to react faster with the more oxygen-rich clusters. It is difficult to say for certain that these trends are opposite because there is insufficient data for the NO reactions. It is interesting that the $Ni_5O_6^-$ cluster reacts significantly more quickly than other reported cluster species with NO and that the trend in the variations reverses for NO_2 reactions at this cluster stoichiometry. Figure 11b gives a comparison of nickel oxide cation reaction rates with NO and NO_2. At first glance the similarities between these two sets of reaction rates appear to be minimal. However, for these reactions, the $Ni_4O_4^+$ clusters react at almost the same rate. Then for both sets of reactions the $Ni_4O_5^+$ clusters react faster than the $Ni_4O_4^+$ clusters. From the $Ni_5O_5^+$ to the $Ni_5O_6^+$ clusters, a decrease in the reaction rates is observed. Finally, an increase in each reaction rate is observed between the $Ni_6O_6^+$ and the $Ni_7O_8^+$ clusters. Figure 11c shows a comparison of the nickel oxide cations and anions reacting with NO_2. As was seen in Figure 10c, the cations and anions again show opposite trends, giving further evidence that charge plays a significant role in reaction rates.

IV. Conclusion

The reaction of nitrogen dioxide with nickel and nickel oxide cluster ions has been presented. Pseudo-first-order bimolecular rate constants for these reactions were also reported. Two major reaction processes are observed for nickel cluster ions, namely, oxidation and addition. Of these, oxidation appears to be the dominant process. For nickel oxide cluster ions addition appears to be the dominant reaction. However, there is some evidence of charge transfer and fragmentation, and with cation oxides further oxidation reactions are observed. Comparisons of measured rate constants reveal interesting similarities between reactions of NO, NO_2, and O_2 with nickel anion clusters. From further comparisons, the importance of charge on reaction rates of both nickel and nickel oxide ions has been shown.

The goal of the work described in each of the parts of this series has been to investigate and develop a greater understanding of reactions between nickel and nickel oxide cluster ions and NO_x gases. In this exploration, gas-phase reactions of nitric oxide and nitrogen dioxide have been carried out. Overall,

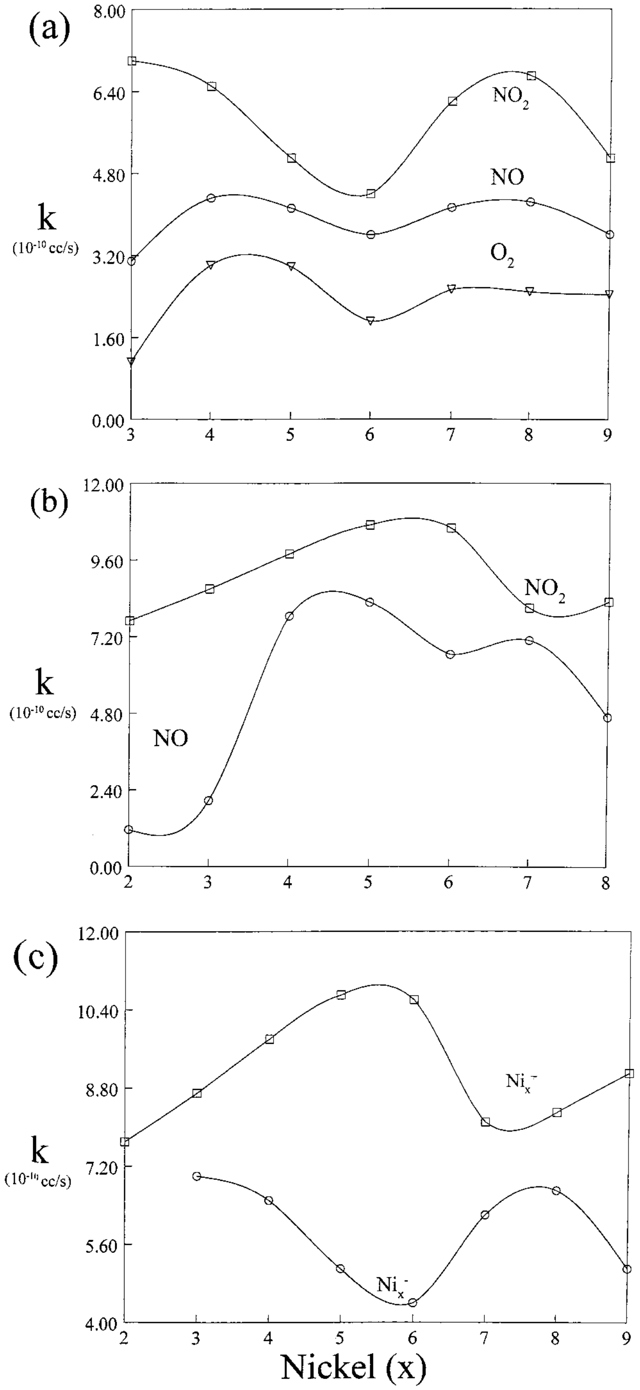

Figure 10. Comparisons of the nickel cluster ion reaction rates from Tables 1 and 2: (a) comparison of nickel anion reaction rates with NO_2, NO, and O_2; (b) comparison of nickel cation reaction rates with NO_2 and NO; (c) comparison of nickel anion and cation reaction rates with NO_2.

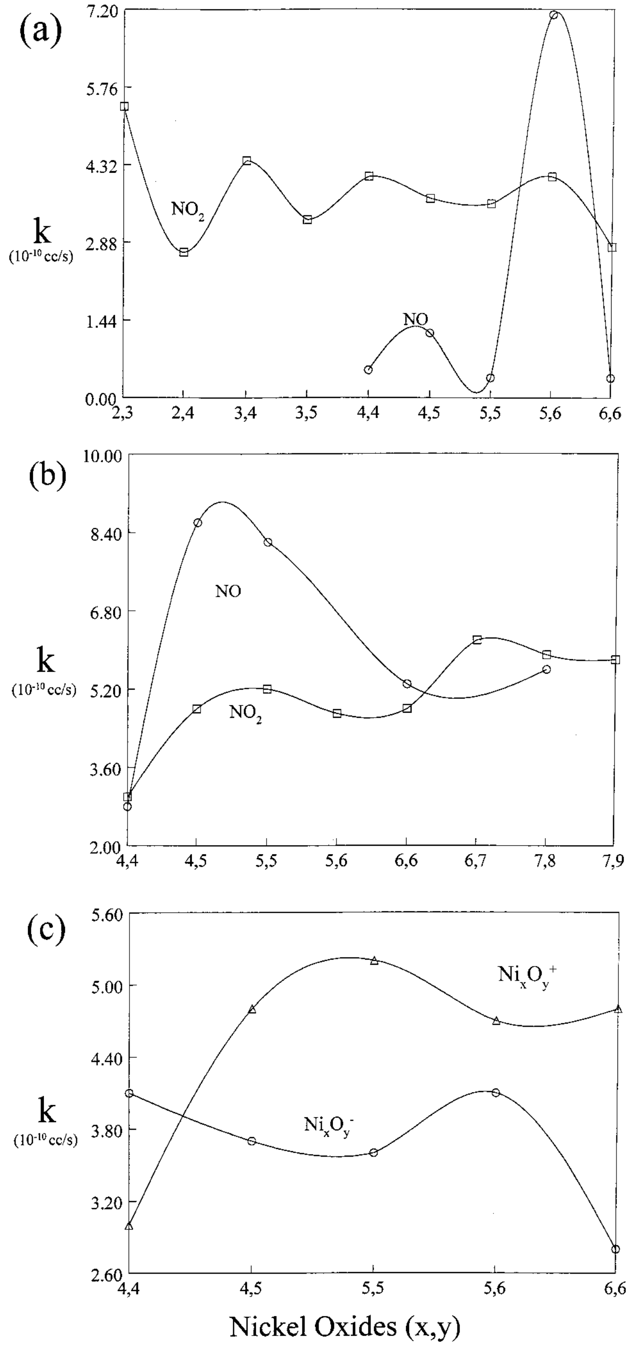

Figure 11. Comparisons of the nickel oxide cluster ion reaction rates from Tables 3 and 4: (a) comparison of nickel oxide anion reaction rates with NO_2 and NO; (b) comparison of nickel oxide cation reaction rates with NO_2 and NO; (c) comparison of nickel oxide anion and cation reaction rates with NO_2.

several different reaction mechanisms have been observed and discussed, many of which are found to be prevalent under several different reaction conditions. Most notable of these reaction mechanisms is the oxidation of nickel cluster ions and in some cases even nickel oxide cation clusters.

The ability of both NO and NO_2 to oxidize nickel cluster is quite interesting. With the exception of nickel cations, where oxidation and NO addition are observed to occur competitively, no NO or NO_2 addition products are observed on the bare nickel cluster ions, indicating that oxidation is the primary reaction process occurring. These initial reaction rates showed that both NO and NO_2 oxidized the clusters faster than O_2. Although it is not as surprising that NO_2 oxidizes nickel clusters more quickly than O_2, it is somewhat surprising that NO also oxidizes these clusters more quickly. Figure 10a shows a comparison of the initial reaction rates for NO, NO_2, and O_2 for nickel anion clusters. From this comparison, it is interesting to observe how cluster size effects carry over from one reaction to another.

Figure 10b shows only a comparison of the reaction rates for NO and NO_2 with nickel cation reactions, because O_2 rate constants for reactions of nickel cation clusters are in some cases an order of magnitude slower. It is most remarkable, for cation nickel clusters, how much slower the reaction rates for O_2 are compared to the rates for both NO and NO_2. The resemblance between the trends in the reaction rates for NO and NO_2 is not quite as noticeable for cations as they are for anions; however, the trends do show some similarities. This again is a further indication that cluster size effects play an important role in reaction processes.

There is no more striking evidence of how cluster size effects contribute to reaction processes than in the fluctuations observed in the reaction rates of oxygen with nickel cations versus cluster size as reported previously in part 3 of this series.[7] These fluctuations indicate an interesting change in reactivity for one cluster size compared to the next. No single factor, geometric or electronic, can easily explain these fluctuations, indicating, as might be expected, a complex interplay between many factors and suggesting that much is yet to be learned before a full understanding of cluster size effects can be developed.

Another significant conclusion from this series of experiments is that of the importance of charge effects on the cluster reactions studied. In parts 1 and 2,[6,7] the reactions of nitric oxide with nickel and nickel oxide anion clusters produced the formation of nitrogen dioxide. In part 3,[5] the reactions of nickel and nickel oxide cation with nitric oxide showed no formation of nitrogen dioxide, indicating that the charge of the cluster in this particular reaction process was a major contributing factor. Part 1 discusses some possible reasons that the charge on the cluster plays such an important role. For instance, the excess electron on the cluster contributes significantly to the local electron density of the reaction center, which may in some way cause a significantly different bonding process to occur. Both cation and anion nickel clusters act to break the nitrogen−oxygen bond to oxidize the cluster. With anions, at some point in the oxidation process the bonding nature changes to facilitate the formation of nitrogen dioxide, perhaps by weakening the nitrogen−oxygen bond instead of breaking it. This also indicates that not only is a charge effect important in this reaction but also stoichiometric effects are crucial. A combination of a negatively charged reaction center and adequate oxygen content for the cluster is responsible for producing nitrogen dioxide from nitric oxide. The importance of stoichiometry can be seen in Figure 11a, where the reaction rates for oxygen-rich nickel oxide are observed to be faster for the reactions of nitric oxide. It is also interesting to note from the same figure that the opposite appears to be the case for many of the reactant species with nitrogen dioxide. That is, when the oxygen content of the cluster increases, the reaction rate decreases (with the exception $Ni_5O_6^-$).

Interesting combined effects of charge, cluster size, and stoichiometry can be seen in Figures 10c and 11c. These two figures show the trends in rates for the reactions of nitrogen dioxide versus stoichiometry and/or cluster size. In each case, opposite trends are observed and cations generally reacted faster than anions. The latter is somewhat unusual considering how much more slowly nickel cations oxidize in the presence on oxygen compared to anions. The oxidation and/or reaction processes occurring between nickel cation clusters and both NO and NO_2 must in some way be substantially different than the oxidation process of nickel cation clusters with oxygen. As mention previously, for anions just the opposite appears to be true; that is, there are striking similarities in the two reaction processes.

As chemists explore the realm of small cluster reactions and compare these reactions to a larger system, a greater understanding of the importance of size, stoichiometry, and charge effects will be needed. With each new system that is explored, we as chemists move closer and closer to developing this overall understanding of reactions of clusters, small particle and localized reactions of larger systems. There is much work yet to be done in the field of cluster science, and there are also numerous future ways in which cluster chemistry can contribute to many other fields of science.

Acknowledgment. Funding provided by the Department of Energy, Grant No. DE-FG02-92ER14258, is gratefully acknowledged.

References and Notes

(1) Castleman, A. W., Jr.; Bowen, K. H, Jr. *J. Phys. Chem.* **1996**, *100*, 12911.

(2) (a) Riley, S. E. In *Metal Ligand Interactions: From Atoms, to Clusters, to Surfaces*; Salahub, D. R., Russo, N., Ed.; Kluwer Academic Press: Dordrecht, 1992; pp 17−36. (b) Eller, K.; Schwarz, H. *Chem. Rev.* **1991**, *91*, 1121.

(3) (a) Fialko, E. F.; Kikhtenko, A. V.; Goncharov, V. B.; Zararaev, K. I. *J. Phys. Chem.* **1997**, *101*, 5772. (b) Shröder, D.; Schwarz, H. *Angew. Chem., Int. Ed. Engl.* **1995**, *34*, 1973.

(4) Shi, Y.; Ervin, K. M. *J. Chem. Phys.* **1998**, *108*, 1757.

(5) Vann, W. D.; Castleman, A. W., Jr. *J. Phys. Chem.*, submitted.

(6) Vann, W. D.; Wagner, R. L.; Castleman, A. W., Jr. *J. Phys. Chem.*, submitted.

(7) Vann, W. D.; Wagner, R. L.; Castleman, A. W., Jr. *J. Phys. Chem.* **1998**, *102*, 1708.

(8) Castleman, A. W., Jr.; Weil, K. G.; Sigsworth, S. W.; Leuchtner, R. E.; Keesee, R. G. *J. Chem. Phys.* **1987**, *86*, 3829.

(9) Corderman, R. R.; Engelking, P. C.; Lineberger, W. C. *J. Chem. Phys.* **1979**, *70*, 4474.

(10) Ho, J.; Polak, M. L.; Ervin, K. M.; Lineberger, W. C. *J. Chem. Phys.* **1993**, *99*, 8542.

(11) Ervin, K. M.; Ho, J.; Lineberger, W. C. *J. Chem. Phys.* **1988**, *89*, 4514.

(12) Gantefor, G.; Gausa, M.; Meiwes-Broer, K.; Lutz, H. *J. Chem. Soc., Faraday Discuss.* **1988**, *86*, 197.

(13) Pacchioni, G.; Chung, S.; Kruger, S.; Rosch, N. *Chem. Phys.* **1994**, *184*, 125.

(14) Hintz, P. A.; Ervin, K. E. *J. Chem Phys.* **1995**, *103*, 7897.

(15) Ervin, K. M.; Ho, J.; Lineberger, W. C. *J. Phys Chem.* **1988**, *92*, 5405.

(16) (a) Pulsing experiments are conducted by interrupting a continuous signal with an electrical pulse at the reactant gas inlet and the sampling orifice. The time difference measured between these two interruptions is the residence time of ions in the reaction zone, under those experimental conditions. (b) MacTaylor, R. S.; Vann, W. D.; Castleman, A. W., Jr. *J. Phys. Chem.* **1996**, *100*, 5329.

(17) Mackay, G. I.; Betowski, L. D.; Payzant, J. D.; Schiff, H. I.; Bohme, D. K. *J. Phys. Chem.* **1976**, *80*, 2919. Su, T.; Chesnavich, W. J. *J. Chem. Phys.* **1982**, *76*, 5183.